# Ginsenoside Rg₃ Inhibits Human Kv1.4 Channel Currents by Interacting with the K531 Residue

**Jun-Ho Lee, Byung-Hwan Lee, Sun-Hye Choi, In-Soo Yoon, Mi Kyung Pyo, Tae-Joon Shin, Woo-Sung Choi, Yoong-Ho Lim, Hyewhon Rhim, Kwang Hee Won, Yong Whan Lim, Han Choe, Dong-Hyun Kim, Yang In Kim, and Seung-Yeol Nah**

*Ginsentology Research Laboratory and Department of Physiology, College of Veterinary Medicine, Konkuk University, Seoul Korea, 143-701 (J.-H.L., B.-H.L., S.-H.C., I.-S.Y., M.K.P., T.-J.S., W.-S.C., S.-Y.N.); Bio/Molecular Informatics Center, Konkuk University (Y.-H.L); Life Science Division, KIST, Seoul Korea 130-701 (H.R.); Department of Physiology and Research Institute for Biomacromolecules, University of Ulsan College of Medicine, Seoul 138-736, Korea (K.H.W., Y.W.L., H.C.); College of Pharmacy Kyung Hee University, 130-701, Korea (D.-H.K); Department of Physiology, Korea University College of Medicine, Seoul 136-705, Korea (Y.I.K.)*

*Running Title*

*Ginsenoside interaction site in human Kv1.4 channels*

**\*Correspondence to**:

Prof. Seung-Yeol Nah, Ginsentology Research Laboratory and Department of Physiology, College of Veterinary Medicine, Konkuk University, Seoul 143-701 Korea.

Tel: 82-2-450-4154; Fax: 82-2-450-3037

**Email: synah@konkuk.ac.kr**

The abbreviations used are: $Rg_3$, ginsenoside $Rg_3$ (20-*S*-protopanaxadiol-3-[O-β-D-glucopyranosyl (1→2)-β-glucopyranoside]); Kv, voltage-gated $K^+$ channel; TEA, tetraethylammonium.

**Manuscript information**

The number of text pages: 34

The number of table: 2

The number of figures: 5

The number of words in abstract: 250

The number of words in introduction: 327

The number of words in discussion: 1515

## ABSTRACT

Recently we demonstrated that the 20($S$) but not the 20($R$) form of ginsenoside $Rg_3$ inhibited $K^+$ currents flowing through Kv1.4 (hKv1.4) channels expressed in *Xenopus* oocytes, pointing to the presence of specific interaction site(s) for $Rg_3$ in the hKv1.4 channel. In the current study, we sought to identify this site(s). To this end, we first assessed how point mutations of various amino acid residues of the hKv1.4 channel affected inhibition by 20($S$)-ginsenoside $Rg_3$ ($Rg_3$). Mutation to K531Y of the K531 residue, which is known to be a key site for $K^+$ activation and to be part of the extracellular tetraethylammonium (TEA) binding site, abolished the $Rg_3$ effect and made the Kv1.4 channel sensitive to TEA applied to the extracellular side of the membrane. Mutations of many other residues, including the pH sensitive-site (H507 to H507Q), were without any significant effect. We next examined whether $K^+$ and TEA could alter the effect of $Rg_3$ and *vice versa*. We found that: 1) raising $[K^+]_o$ reduced the inhibitory effect of $Rg_3$ on hKv1.4 channel currents, while $Rg_3$ shifted the $K^+$ activation curve to the right and 2) TEA caused a rightward shift of the $Rg_3$ concentration-response curve of wild-type hKv1.4 channel currents, whereas $Rg_3$ caused a rightward shift of the TEA concentration-response curve of K531Y mutant channel currents. The docked modeling revealed that K531 residue plays a key role in forming hydrogen bonds between $Rg_3$ and hKv1.4 channels. These results indicate that $Rg_3$ inhibits the hKv1.4 channel current by interacting with residue K531.

Voltage-gated $K^+$ (Kv) channels play critical roles in a wide variety of physiological processes, including the regulation of neurotransmitter release, neuronal excitability, heart rate, muscle contraction, hormone secretion, epithelial electrolyte transport, cell volume, and cell proliferation in neuronal and non-neuronal cells (Hille, 2001). Kv channels consist of tetramers of pore-forming Kvα and auxiliary Kvβ subunits (Hille, 2001). The Kvα subunit is composed of six α-helical transmembrane segments (S1-S6). The S4 segment acts as the voltage-sensing apparatus of the $K^+$ channel (Hille, 2001), while the pore-forming S5-S6 segments constitute a selectivity filter and govern voltage-dependent increases in $K^+$ permeability. Site-directed mutagenesis studies using Kvα subunits have clarified the detailed action and binding sites of various drugs that regulate Kv channel activity (Hille, 2001). Some Kv channel α subunits exhibit transient A-type $K^+$ currents and N-type inactivation, and others, long-lasting delayed rectifying C-type $K^+$ currents and C-type inactivation, depending on their channel conductance and gating characteristics (Patel and Campbell, 2005).

Ginseng, the root of *Panax ginseng* C.A. Meyer, is well known in herbal medicine as a tonic and restorative agent, and it is consumed widely around the world. The molecular bases of ginseng's actions are largely unknown. Numerous reports have suggested that the main molecular ingredients responsible are ginsenosides (also called ginseng saponins), amphiphilic molecules consisting of a hydrophobic aglycone backbone (a hydrophobic four-ring steroid-like structure) linked to monomeric, dimeric

or tetrameric hydrophilic carbohydrate side chains (Fig. 1) (Nah, 1997). However it is unclear how ginsenosides produce their pharmacological effects. Recently we reported that ginsenoside $Rg_3$ (20-*S*-protopanaxadiol-3-[O-β-D-glucopyranosyl (1→2)-β-glucopyranoside]) ($Rg_3$) had an inhibitory effect on voltage-dependent human Kv1.4 (hKv1.4) channel activity expressed in *Xenopus laevis* oocytes (Jeong et al., 2004). In this report we present evidences that $Rg_3$ interacts with residue K531 to inhibit the channel currents. In addition, the docked modeling studies using hKv1.4 channels support that K531 residue plays an important role in the $Rg_3$-mediated regulations of hKv1.4 channel by forming hydrogen bonds between $Rg_3$ and hKv1.4 channels.

## Materials and Methods

**Materials** Ginsenosides were kindly provided by the Korean Ginseng Cooperation (Taejon, Korea). The cDNA for human $K^+$ channel Kv1.4 (Gene bank ID: NM_002233) was kindly provided by Dr. Pongs (University of Hamburg, Germany). Other agents were purchased from Sigma-Aldrich (St. Louis, MO, USA).

**Preparation of Xenopus oocytes and microinjection** *Xenopus laevis* frogs were purchased from Xenopus I (Ann Arbor, MI, USA). Their care and handling were in accordance with the highest standards of institutional guidelines. For isolation of

oocytes, frogs were anesthetized with an aerated solution of 3-amino benzoic acid ethyl

ester and the ovarian follicles were removed. The oocytes were separated with

collagenase followed by agitation for 2 h in $Ca^{2+}$-free medium containing 82.5 mM

NaCl, 2 mM KCl, 1 mM $MgCl_2$, 5 mM HEPES, 2.5 mM sodium pyruvate, 100 units/ml

penicillin and 100 µg/ml streptomycin. Stage V-VI oocytes were collected and stored in

ND96 medium (in mM: 96 NaCl, 2 KCl, 1 $MgCl_2$, 1.8 $CaCl_2$, and 5 HEPES, pH 7.5)

supplemented with 0.5 mM theophylline and 50 µg/ml gentamicin. The oocyte-

containing solution was maintained at 18°C with continuous gentle shaking and

renewed every day. Electrophysiological experiments were performed within 5-6 days

of oocyte isolation, with chemicals applied to the bath. For $K^+$ channel experiments, Kv

channel-encoding cRNAs (40 nl) were injected into the animal or vegetal pole of each

oocyte one day after isolation, using a 10 µl microdispenser (VWR Scientific, San

Francisco, CA, USA) fitted with a tapered glass pipette tip (15-20 µm in diameter) (Lee

et al., 2005).

**Site-directed mutagenesis of the Kv1.4 α subunit and *in vitro* transcription of**

**Kv1.4 channel cDNAs** Single or double amino acid substitutions were made using a

QuikChange[TM] XL Site-Directed Mutagenesis Kit (Stratagene, La Jolla, CA, USA),

along with Pfu DNA polymerase and sense and antisense primers encoding the desired

6

mutations. Overlap extension of the target domain by sequential polymerase chain reaction (PCR) was carried out according to the manufacturer's protocol. The final PCR products were transformed into *E. coli* strain DH5α, screened by PCR and confirmed by sequencing of the target regions. The mutant DNA constructs were linearized at their 3' ends by digestion *with Xho*I, and run-off transcripts were prepared using the methylated cap analog, $m^7G(5')ppp(5')G$. The cRNAs were prepared using a mMessage mMachine transcription kit (Ambion, Austin, TX, USA) with T7 RNA polymerase. The absence of degraded RNA was confirmed by denaturing agarose gel electrophoresis followed by ethidium bromide staining. Similarly, recombinant plasmids containing Kv channel cDNA inserts were linearized by digestion with the appropriate restriction enzymes, and cRNAs were obtained using the mMessage mMachine *in vitro* transcription kit with SP6 RNA polymerase or T7 polymerase. The final cRNA products were resuspended at a concentration of 1 µg/µl in RNase-free water, and stored at –80°C (Lee et al., 2005).

**Data recording** A custom-made Plexiglas net chamber was used for two-electrode voltage-clamp recordings as previously reported (Lee et al., 2005). The oocytes were impaled with two microelectrodes filled with 3M KCl (0.2-0.7 MΩ), and electrophysiological experiments were carried out at room temperature using an Oocyte Clamp (OC-725C, Warner Instruments, Hamsden, CT, USA). Stimulation and data

acquisition were controlled with a pClamp 8 (Axon Instruments, Union City, CA, USA).

For most electrophysiological experiments, oocytes were perfused initially with ND96

solution (in mM: 96 NaCl, 3 KCl, 2 CaCl$_2$, 5 HEPES, pH 7.4 with NaOH) and control

current recordings were obtained. To measure K$^+$ activation of the Kv1.4 channel, a

solution was applied in which the NaCl was replaced with various concentrations of

KCl. In all cases the solution was perfused at a flow rate of ≈3 ml/min, and the system

was allowed 30 to 60 s to reach steady state prior to current recording. The oocytes were

then clamped at a holding potential of –80 mV, membrane potential was depolarized to

+50 mV for 500 ms every 10 s, and currents were recorded.

**Homology modeling.** A homology model of the hKv1.4 was built on the basis

of the 2.9 Å crystal structure of the rat Kv1.2 channel (PDB ID code: 2A79), using the

homology modeling program, MODELLER 8v2 (Sali and Blundell, 1993). Sequence

alignment was carried out using the AlignX module of the Vector NTI (Lu and

Moriyama, 2004). A stretch of amino acids in the Kv1.2 channel corresponding to the

region from M438 to T571 in hKv1.4 was chosen as the template for homology

modeling, because the other regions had structures missing in the PDB file. The chosen

region contained the pore and its neighboring areas, and the sequence identity between

hKv1.4 with rat Kv1.2 through this region was ~90%. The homotetrameric structure

was restrained to maintain symmetry during homology modeling. A total of 200

structures were generated, and the one with the lowest DOPE score from MODELLER

was chosen for further minimization. Hydrogen atoms were added to the homology

model using Sybyl v7.0 (Tripos Inc., St. Louis, MO, USA). The homology model

structure was energy-minimized using the Tripos forcefield protocol in Sybyl. The same

strategies were used to generate a homology model of K531Y.

**Virtual docking.** The structure of $Rg_3$ was constructed using Chemdraw ultra 8.0

(Cambridgesoft, Cambridge, MA, USA) and converted to a 3-dimensional model and

energy minimized using Chem3D ultra 8.0 (Cambridgesoft, Cambridge, MA, USA),

followed by a second round of energy minimization using Sybyl forcefield. The virtual

dockings of $Rg_3$ to the homology model of hKv1.4 wild-type and K531Y mutant

channels were performed using GOLD v3.0 (The Cambridge Crystallographic Data

Centre, Cambridge, UK), a program that uses stochastic genetic algorithms for

conformational searching (Verdonk et al., 2003). The K531 residues in each of the four

subunits were designated as the active site residues, and the active radium was set as 10

Å from the active site residues. The docked models with the best GOLD scores were

selected for final complex structural analysis. The interactions between the ligand and

each homology model were examined using the SILVER tool of the GOLD software

package. All structural figures were prepared using PyMol v0.98 (DeLano Scientific

LLC, San Francisco, CA, USA).

**Data analysis** To obtain the concentration-response curve of the effect of $Rg_3$ on the $K^+$

current from the hKv1.4 channel, the peak amplitudes at different concentrations of $Rg_3$

were plotted, and Origin software (Origin, Northampton, MA, USA) was used to fit the

plot to the Hill equation: $y/y_{max} = [A]^{nH}/([A]^{nH} + [IC_{50}]^{nH})$, where y is the peak current at

a given concentration of $Rg_3$, $y_{max}$ is the maximal peak current, $IC_{50}$ is the concentration

of $Rg_3$ producing a half-maximal effect, [A] is the concentration of $Rg_3$, and nH is the

Hill coefficient. All values are presented as means ± S.E.M. The significance of

differences between mean control and treatment values was determined using Student's

*t*-test. $P < 0.05$ was considered statistically.

## Results

### $Rg_3$ inhibits hKv1.4 channel currents more potently than other ginsenosides.

Using the two-electrode voltage-clamp technique we recorded hKv1.4 channel currents

from *Xenopus* oocytes injected with cRNA encoding the hKv1.4 channel protein. To

elicit the currents, we applied a voltage step (500-ms duration) to +50 mV at 10-s

intervals from a holding potential of –80 mV. The currents evoked by this voltage-clamp

protocol were transient A-type $K^+$ currents that decayed rapidly (Fig. 1B, *inset*)

(Gomez-Hernandez et al., 1997). $Rg_3$, at 100 μM inhibited the hKv1.4 channel currents

by an average of 65%, and other ginsenosides ($Rb_1$, Rc, Rd, Rf, $Rg_1$, $Rh_2$, CK) were

much less effective (Fig. 1B). The $Rg_3$ current effect was concentration-dependent (Fig.

2A) and reversible (data not shown). The $IC_{50}$ value and Hill coefficient were 32.6 ±2.2

μM and 1.59 ± 0.13, respectively (Table 1).

To assess the effect of $Rg_3$ on the current-voltage (I-V) relationship, we

constructed I-V curves with and without $Rg_3$ in the bath. The current responses evoked

by voltage steps (i.e., a series of voltage pulses of 500-ms duration given in 10-mV

increments and 10-s intervals from the holding potential of –80 mV) were used to

construct the I-V curve. In the absence of $Rg_3$, hKv1.4 currents were elicited by voltage

pulses more positive than –40 mV, and current amplitude increased linearly with further

depolarization (Fig. 2D). The presence of $Rg_3$ reduced current amplitude over the entire

voltage range in which the current was activated (Fig. 2D).

**The K531Y substitution affects $Rg_3$ inhibition of channel current**. Previous

works showed that $Rg_3$ inhibited hvKv1.4 channel current in a stereospecific manner

(Jeong., 2004) and that $Rg_3$ regulates $5\text{-}HT_{3A}$ receptor channel activity through

interaction with amino acid residues in the channel pore region (Lee et al., 2007). We

therefore hypothesized that $Rg_3$ might have a specific interaction site(s) on the hKv1.4

channel and that $Rg_3$ interaction site(s) with the hKv1.4 channel might be related with

channel pore region. To identify that site(s), we first made the following changes by

site-directed mutations in channel pore regions: channel pore sites (S510 to S510K,

D513 to D513Q, V525 to V525L and V535 to V535Q), outer pore sites (K531 to

K531A, P532 to P532A, I533 to I533A, T534 to T534A and V535 to V535A). Next, we

also constructed mutant channels as follows: N-glycosylation site (N352 to N353Q)

(Watanabe et al., 2004), voltage sensor site (R447 to R447C and R450 to R450C)

(Fedida and Hesketh, 2001), voltage shift sites (L478 to L478F and G548 to G548P)

(Judge et al., 1999; Magidovich and Yifrach, 2004), pH sensitive site (H507 to H507Q)

(Claydon et al., 2004) and C-type inactivation site (V560 to V560A) (Bett and

Rasmusson, 2004). We found that one of outer pore residues K531A substitution

significantly attenuated $Rg_3$ inhibition of the hKv1.4 channel currents (Fig. 2A), while

the other changes had no significant effects (Table 1). These results showed a possibility

that $Rg_3$ regulates hKv1.4 channel activity by interacting with K531, which is also

known as one of $K^+$ activation sites. Therefore, we constructed mutant channels at $K^+$

activation sites (K531 to K531Y, I533 to I533M, and K531-I533 to K531Y-I533M)

(Pardo et al., 1992; Claydon et al., 2004). We found that the K531Y substitution and the

K531Y-I533M double substitution almost abolished $Rg_3$ inhibition of the hKv1.4

channel currents (Fig. 2B-D). These results indicate that $Rg_3$-induced regulation of

hKv1.4 channel activity is closely related with K531 residue.

**Extracellular $K^+$ and $Rg_3$ antagonize each other's effect on hKv1.4 channel**

**currents.** If indeed $Rg_3$ produces its effect by interacting with K531, the $K^+$ activation

site, an increase in extracellular $[K^+]_o$ would compete with $Rg_3$ for K531 and thus inhibit

the action of the ginsenoside. Conversely, $Rg_3$ would inhibit $K^+$ activation by competing

with $K^+$ for K531. We found that extracellular $K^+$ and $Rg_3$ indeed antagonized each

other's effect. Figure 3A-C shows that raising extracellular $[K^+]_o$ inhibited the effect of

$Rg_3$ ($IC_{50}$ of extracellular $K^+$ for the $Rg_3$ effect: $6.4 \pm 2.9$ mM), while Figure 3D shows

that $Rg_3$ (100 μM) inhibited the effect of $K^+$, thus shifting the $K^+$ activation curve to the

right ($EC_{50}$s of $K^+$ before and after $Rg_3$ treatment: $4.2 \pm 0.9$ mM and $9.2 \pm 1.5$ mM,

respectively; $P < 0.01$). These findings, confirm that $Rg_3$ competes with extracellular

$[K^+]$ for the K531 residue.

**TEA and $Rg_3$ inhibit each other's effect on hKv1.4 channel currents.**

Residue K531 is also known to form a part of the extracellular binding site for TEA

(Heginbotham and Mackinnon, 1992; Gomez-Hernandez et al., 1997). We therefore

reasoned that, if $Rg_3$ produced its effect by interacting with K531, extracellular

13

application of TEA should antagonize the effect of $Rg_3$ on channel currents, and

conversely, $Rg_3$ should antagonize the TEA effect. To test these possibilities we used

oocytes expressing wild-type or K531Y mutant hKv1.4 channels, because

extracellularly applied TEA binds to both types of channel but only inhibits the mutant

channels (Fig. 4A; $IC_{50}$: $26.5 \pm 2.6$ µM). Fig. 4B shows that TEA had no effect by itself

on wild-type hKv1.4 channel currents, but that it inhibited the action of $Rg_3$, thus

causing the $Rg_3$ concentration-response curve to shift to the right ($IC_{50}$s of $Rg_3$ before

and during 10-µM TEA treatment: $35.1 \pm 3.6$ µM and $93.1 \pm 6.7$ µM, respectively; $P <$

$0.001$). Conversely $Rg_3$ antagonized the effect of TEA on K531Y channel currents,

causing a rightward shift of the TEA concentration-response curve ($IC_{50}$'s of TEA

before and during 100-µM $Rg_3$ treatment: $23.3 \pm 2.7$ µM and $40.1 \pm 7.1$ µM,

respectively; $P < 0.01$) (Fig. 4C). These results lend further support to the hypothesis

that $Rg_3$ interacts with K531 to inhibit hKv1.4 channel currents.

**Docked modeling of interactions between $Rg_3$ and the hKv1.4 channel.** To

further examine the possible interaction mode between $Rg_3$ and the hKv1.4 channel, we

carried out homology modeling of wild-type and K531Y mutant hKv1.4 channels. Our

model was generated using the MODELLER program and the crystal structure of

hKv1.2. Virtual docking of $Rg_3$ to the homology models was performed using the

docking program, GOLD. Interestingly, the best-fit docking results showed that $Rg_3$ forms six hydrogen bonds with wild-type hKv1.4 channels but only two hydrogen bonds with K531Y mutant channels (Fig. 5 and Table 2). In the wild-type channel, the first carbohydrate coupled to the $Rg_3$ backbone forms two hydrogen bonds with K531 of domain I (designated as Roman numeral I) and one hydrogen bond with H507 (IV). The second carbohydrate of $Rg_3$ forms one hydrogen bond with K531 (I), one hydrogen bond with T505 (I) and one hydrogen bond with H507 (I). In the K531Y mutant channel, the second carbohydrate of $Rg_3$ forms one hydrogen bond with Y531 (I) and the first carbohydrate of $Rg_3$ forms a hydrogen bond with H507 (IV) (Fig. 5 and Table 2). Notably, the wild-type Kv1.4 channel pore is blocked by the hydrophobic triterpenoid backbone moiety of $Rg_3$. The mutant channel is also blocked by $Rg_3$, but the low affinity of $Rg_3$ to the mutant channel (inferred from the small number of hydrogen bonds) might result in ineffective blocking of the mutant channel by $Rg_3$, thus accounting for the inability of $Rg_3$ to inhibit K531Y mutant channel currents.

## Discussion

The Kv1.4 channel is a transient A-type or rapidly inactivating Kv channel. Kv1.4 channels are mainly located at axon and pre-synaptic terminals (Cooper et al.,

1998; Alonso and Widmer, 1997; Hoffman and Johnston, 1998; Adams et al., 2000), and

function to modulate action potential waveforms and neurotransmitter release (Debanne

et al., 1997; Jackson et al., 1991). They also affect the amplitude of the plateau phase

and duration of action potentials in ventricular myocytes (Campbell et al., 1993; Patel

and Campbell, 2005). Thus, these channels are one of the targets of drugs for treatment

of pathologic conditions including cardiac arrhythmia. We previously demonstrated that

$Rg_3$ regulated hKv1.4 channel currents in a stereospecific manner (Jeong et al., 2004).

However, very little was known of its molecular mechanism of action.

In the present study we observed that mutation of K531 to K531A or K531Y, as

well as raising extracellular $[K^+]_o$ from 3 to 99 mM, attenuated or almost abolished $Rg_3$

inhibition of hKv1.4 channel currents. These results show a possibility that $Rg_3$ might

interacts with the $K^+$ activation sites, H507, K531, and I533 (Pardo et al., 1992;

Claydon et al., 2004). To test these possibilities, we examined the effects of $Rg_3$ on

H507Q, K531Y, I533M and K531Y-I533M channels. As shown in Figure 2, $Rg_3$ did not

inhibit K531Y and K531Y-I533M channels even at high concentrations, whereas its

effect on H507Q and I533M mutant channels was similar to that seen with wild-type

channels (Table 1). These results indicate that although both H507 and I533 are

involved in $K^+$ activation (Pardo et al., 1992; Claydon et al., 2004), they are not

involved in $Rg_3$ regulation of channel activity. This view was supported by the results

from our double mutation experiments. Furthermore, mutations in the channel pore

region, pH-sensitive sites, voltage sensor and other regulatory sites did not affect $Rg_3$

inhibition (Table 1). Interestingly, $Rg_3$ is not structurally similar to TEA, a well-known

$K^+$ channel blocker that can function on either side of the cell membrane. In contrast to

TEA, $Rg_3$ does not have any charged groups apart from the hydroxyls of its

carbohydrate and backbone structures (Fig. 1A). Despite the structural difference

between $Rg_3$ and TEA, we found that the K531Y mutation of amino acid 531, which

forms part of the external TEA interaction site, almost abolished $Rg_3$ inhibition of the

channel currents. We also showed that $Rg_3$ competes with TEA for inhibition of K531Y

channel currents (Fig. 4B) and vice versa (Fig. 4C). Interestingly, the rightward shift of

the $Rg_3$ concentration-response curve caused by TEA in wild-type channels was

stronger than that of the TEA concentration-response curve caused by $Rg_3$ in K531Y

channels. Thus by making use of the fact that K531Y channels are sensitive to TEA

whereas wild-type channels are not, we were able to demonstrate that $Rg_3$ may be an

allosteric interaction site for TEA and $Rg_3$. However, it is unlikely that $Rg_3$ exhibits an

allosteric interaction with TEA on the intracellular surface of the channel since we have

shown that $Rg_3$ regulates channels from the outside not the inside in out-side out patch

clamp experiments (Lee et al., 2004).

MacDonald et al (1998) showed that *n*-alkyl sulphate anions but not TEA inhibit wild-type rat Kv1.4 channel currents and that mutation of K533 to K533Y rendered channels sensitive to TEA but insensitive to *n*-alkyl sulphate anions. This indicates that K533 may play a role in *n*-alkyl sulphate anion-mediated Kv1.4 channel regulation via the external TEA interaction site. In addition, Zaks-Makhina et al. (2004) and Salvador-Recatala et al. (2006) have studied a neuroprotective compound, called 48F10, from yeast. They showed that 48F10 inhibited R476Y mutant rat Kv1.5 channel currents, (R476 is analogous to K531 in hKv1.4 channel) and wild-type rat Kv2.1 channel currents via the external TEA interaction site, since the presence of external TEA greatly reduced 48F10 current inhibition. Taken together, the previous and present observations raise the possibility that a lysine or analogous amino acid residue in the outer pores of subsets of Kv channels not only forms part of the external TEA interaction site but also plays a role as an allosteric interaction or overlapping site for TEA and certain other compounds.

Ginsenosides have effects on multiple targets (Attele et al., 1999). We and others have reported that ginsenosides, including $Rg_3$, also act on various ion channels at pre- and post-synaptic sites in the nervous systems and inhibit neurotransmitter release (Choi

et al., 2003; Kim et al., 2002; Lee et al., 2005; Liu et al., 2001; Nah et al., 1995; Sala et al., 2002; Tachikawa et al., 2001). Thus it appears that ginsenosides show a low degree of selectivity for ion channels compared to drugs or toxins that act on particular ion channels. However, we were not able to clearly define and comprehend the molecular mechanisms underlying ginsenoside-mediated regulation of multiple ion channels. We demonstrated that $Rg_3$ regulates $5\text{-}HT_{3A}$ receptor channel activity in the open state through interactions with amino acids such as V291, F292 and I295 in the gating pore region of transmembrane domain 2 (Lee et al., 2007). In the present study, we found that $Rg_3$ regulates Kv1.4 channel activity through interaction with the outer pore K531 residue and may interact allosterically with the external TEA binding site. Thus $Rg_3$ affects $5\text{-}HT_{3A}$ receptors and Kv1.4 channel activity via different interaction sites and different modes of regulation.

We next sought to examine the possible mechanisms underlying $Rg_3$-induced hKv1.4 channel activity regulation. As shown in Figure 1A, $Rg_3$ consists of a carbohydrate portion, a steroid backbone and an alkene side chain. To determine how $Rg_3$ interacts with Kv1.4 channels, we performed docked modeling experiments using wild-type and K531Y mutant channels. Our docked modeling study revealed that the two carbohydrates of $Rg_3$ could form six hydrogen bonds with residues T505 (I), H507

(I), H507 (IV) and K531 (I) in the wild-type channel. We previously demonstrated that

$Rg_3$ regulates ligand-gated ion channels at the extracellular but not intracellular side

using out-side out patch clamp method (Lee et al., 2004) and that modifications or

removal of the carbohydrate portion of $Rg_3$ abolished $Rg_3$-mediated ion channel

regulations, but at the time we were unable to explain exactly how $Rg_3$ regulates ion

channel activity from the extracellular side and the carbohydrate portion of $Rg_3$ was

involved in ion channel regulations (Kim et al., 2005). The modeling results in our

present study suggest that the previously examined carbohydrate modifications might

induce a conformational change in $Rg_3$ and/or prevent the formation of hydrogen bonds

between $Rg_3$ and the critical residues. In the present study, the K531Y mutation was

found to induce a conformational change in the channel protein (Fig. 5C), resulting in

the formation of only two hydrogen bonds between $Rg_3$ and amino acid residues at the

pore entryway. Thus, loss of hydrogen bonding between $Rg_3$ and the channel outer pore,

whether through mutation or carbohydrate modification, appears to decrease the binding

affinity of $Rg_3$, resulting in loss of $Rg_3$-induced channel regulation. Furthermore, as

shown Figure 5B, our modeling revealed that the triterpenoid backbone of $Rg_3$ blocks

the channel pore when the proper hydrogen bonds are formed; this may provide a

secondary level of $Rg_3$-induced inhibition of outward $K^+$ currents following

20

depolarization. Future studies will be necessary to determine the exact roles of the carbohydrates and/or triterpenoid backbone structures of $Rg_3$ in terms of Kv1.4 channel regulation.

We may ask whether the *in vitro* $Rg_3$ inhibition of the hKv1.4 channel applies also to its *in vivo* pharmacological effects. Ginseng has many beneficial effects on the cardiovascular systems (Gillis, 1997). Gao et al. (1992) have shown that ginsenoside administration via the intravenous route attenuates ischemic and reperfused arrhythmia in rats, and Yang et al. (1999) showed that ginsenoside administration via the intraperitoneal route attenuates myocardial reperfusion arrhythmia in rats fed a high cholesterol diet. Anti-arrhythmic agents such as quinidine block anti-arrhythmic effects on Kv1.4 and other cloned $K^+$ channels (Wang et al., 2003) but we do not have any direct evidence that $Rg_3$-mediated Kv1.4 channel regulation can be used prophylactically or therapeutically against arrhythmia as quinidine can. More investigation is needed of the potential application of $Rg_3$ to heart dysfunction. In addition, Kim et al. (1999a and 1999b) showed that $Rg_3$ induced relaxation of the rat aorta via endothelium-dependent and -independent routes. They further showed that $K^+$ channels in the rat aorta might be involved in the effect of $Rg_3$, since $Rg_3$-mediated aorta relaxation was achieved in a TEA-sensitive manner.

In summary, we have used site-directed mutagenesis, $K^+$ activation experiments, and analysis of the external TEA interaction site to further characterize $Rg_3$ regulation of hKv1.4 channel activity. We found that the K531 residue of the hKv1.4 channel is involved in $Rg_3$-mediated Kv1.4 channel regulation and that $Rg_3$ may interact allosterically with the external TEA binding site via residue K531. Furthermore, in a molecular modeling we showed for the first time that two carbohydrates of $Rg_3$ interact with amino acid residues, including K531, through the formation of hydrogen bonds, which are decreased in K531Y mutant channels. These novel findings provide insight into the pharmacological basis of the beneficial effects of ginseng on cardiovascular systems.

# References

Adams JP, Anderson AE, Varga AW, Dineley KT, Cook RG, Pfaffinger PJ, and Sweatt JD (2000) The A-type potassium channel Kv4.2 is a substrate for the mitogen-activated protein kinase ERK. *J Neurochem* **75**:2277-2287

Alonso G and Widmer H (1997) Clustering of Kv4.2 potassium channels in postsynaptic membrane of rat supraoptic neurons: an ultrastructural study. *Neuroscience* **77**:617-621

Attele AS, Wu JA, Yuan CS (1999) Ginseng pharmacology: multiple constituents and multiple actions. *Biochem Pharmacol*. **58**: 1685-1693

Bett GC and Rasmusson RL (2004) Inactivation and recovery in Kv1.4 $K^+$ channels: lipophilic interactions at the intracellular mouth of the pore. *J Physiol* **556**:109-120

Campbell DL, Rasmusson RL, Qu Y, Strauss HC (1993) The calcium-independent transient outward potassium current in isolated ferret right ventricular myocytes. I. Basic characterization and kinetic analysis. *J Gen Physiol* **101**:571-601

Choi S, Lee JH, Oh S, Rhim H, Lee SM, and Nah SY (2003) Effects of ginsenoside $Rg_2$ on the 5-HT3A receptor-mediated ion current in Xenopus oocytes. *Mol. Cells* **15**: 108-113.

Claydon TW, Makary SY, Dibb KM, and Boyett MR (2004) $K^+$ activation of

kir3.1/kir3.4 and kv1.4 K$^+$ channels is regulated by extracellular charges. *Biophysical J* **87**:2407-2418

Cooper EC, Milroy A, Jan YN, Jan LY, and Lowenstein DH (1998) Presynaptic localization of Kv1.4-containing A-type potassium channels near excitatory synapses in the hippocampus. *J Neurosci* **18**:965-974

Dascal N (1987) The use of Xenopus oocytes for the study of ion channels. *CRC Crit. Rev. Biochem.* **22**: 317-387.

Debanne D, Guerineau NC, Gahwiler BH, and Thompson SM (1997) Action-potential propagation gated by an axonal I(A)-like K$^+$ conductance in hippocampus. *Nature* **389**:286-289

Fedida D and Hesketh JC (2001) Gating of voltage-dependent potassium channels. *Prog Biophys Mol Biol* **75**:165-199

Gao BY, Li XJ, Liu L, and Zhang BH (1992) Effect of panaxatriol saponins isolated from Panax notoginseng (PTS) on myocardial ischemic arrhythmia in mice and rats. *Yao Xue Xue Bao*. **27**:641-644

Gillis, CN (1997) *Panax* ginseng pharmacology: a nitric oxide link? *Biochem Pharmacol*. **54**: 1-8.

Gomez-Hernandez JM, Lorra C, Pardo LA, Stuhmer W, Pongs O, Heinemann SH, and

Elliott AA (1997) Molecular basis for different pore properties of potassium channels from the rat brain Kv1 gene family. *Pflugers Arch* **434**:661-668

Hille B (2001) Ion channels of excitable membranes. *Sinauer Associates, Inc, Sunderland, MA*

Heginbotham L and Mackinnon R (1992) The aromatic binding site for tetraethylammonium ion on potassium channels. *Neuron* **8**:483-491

Hoffman DA and Johnston D (1998) Downregulation of transient $K^+$ channels in dendrites of hippocampal CA1 pyramidal neurons by activation of PKA and PKC. *J Neurosci* **18**:3521-3528

Jackson MB, Konnerth A, and Augustine GJ (1991) Action potential broadening and frequency-dependent facilitation of calcium signals in pituitary nerve terminals. *Proc Natl Acad Sci USA* **88**:380-384

Jeong SM, Lee JH, Kim JH, Lee BH, Yoon IS, Lee JH, Kim DH, Rhim H, Kim Y, and Nah SY (2004) Stereospecificity of ginsenoside $Rg_3$ action on ion channels. *Mol Cells* **18**:383-389

Judge SI, Monteiro MJ, Yeh JZ, and Bever CT (1999) Inactivation gating and 4-AP sensitivity in human brain Kv1.4 potassium channel. *Brain Res* **831**:43-54

Kang DI, Lee JY, Yang JY, Jeong SM, Lee JH, Nah SY, and Kim Y (2005) Evidence that

the tertiary structure of 20(S)-ginsenoside Rg3 with tight hydrophobic packing near the chiral center is important for Na+ channel regulation. Biochem Biophysic Res Communi 333:1194-1201.

Kim JH, Hong YH, Lee JH, Kim DH, Jeong SM, Lee BH, Lee SM, and Nah SY (2005) A role for the carbohydrate portion of ginsenoside $Rg_3$ in $Na^+$ channel inhibition. *Mol Cells* **19**:137-142

Kim ND, Kang SY, Kim MJ, Park JH, and Schini-Kerth VB (1999a) The ginsenoside $Rg_3$ evokes endothelium-independent relaxation in rat aortic rings: role of $K^+$ channels. *Eur J Pharmacol* **367**: 51-57

Kim ND, Kang SY, Park JH, and Schini-Kerth VB (1999b) Ginsenoside $Rg_3$ mediates endothelium-dependent relaxation in response to ginsenosides in rat aorta: role of $K^+$ channels. *Eur J Pharmacol* **367**: 41-49

Kim S, Ahn K, Oh TH, Nah SY, and Rhim H (2002) Inhibitory effect of ginsenosides on NMDA receptor-mediated signals in rat hippocampal neurons. *Biochem. Biophys. Res. Commun*. **296**: 247-254.

Lee JH, Jeong SM, Kim JH, Lee BH, Yoon IS, Lee JH, Choi SH, Kim DH, Rhim H, Kim S, Kim JI, Jang CG, Song JH, and Nah SY (2005) Characteristics of ginsenoside $Rg_3$-mediated brain $Na^+$ current inhibition. *Mol Pharmacol* **68**:1114-1126

Lee BH, Jeong SM, Ha TS, Park CS, Lee JH, Kim JH, Kim DH, Han JS, Kim, HC, Ko SR, and Nah SY (2004) Ginsenosides Regulate Ligand-gated Ion Channels from the Outside. *Mol Cells* **18:** 115-121

Lee BH, Lee JH, Lee SM, Yoon IS, Lee JH, Choi SH, Pyo MK, Rhim H, Kim HC, Jang CG, Lee BC, Park CS, and Nah SY (2007) Identification of ginsenoside interaction sites in 5-HT$_{3A}$ receptors. *Neuropharmacology* **52:** 1139-1150

Liu D, Li B, Liu Y, Attele, AS, Kyle JW, and Yuan CS (2001) Voltage-dependent inhibition of brain Na$^+$ channels by American ginseng. *Eur J Pharmacol* **413**: 47-54

Lu G and Moriyama EN (2004) Vector NTI, a balanced all-in-one sequence analysis suite. *Briefings in bioinformatics* **5**:378-388

Magidovich E and Yifrach O (2004) Conserved gating hinge in ligand- and voltage-dependent K$^+$ channels. *Biochemistry* **43**:13242-13247

McAllister RE and Noble D (1966) The time and voltage dependence of the slow outward current in cardiac Purkinje fibres. *J Physiol* **186**:632-662

MacDonal S, Elliott AA, Harrold JA, and Elliott JR (1998) Influence of outer pore residue K533 on the inhibition of Kv1.4 potassium channel s by n-alkyl sulphate anions. *Pflugers Arch*. **436**: 623-626

Nah SY (1997) Ginseng : Recent Advances and Trends. *Kor. J. Ginseng Sci*. **21**: 1-12.

Nah, SY, Park, HJ, and McCleskey, EW. (1995) A trace component of ginseng that inhibits $Ca^{2+}$ channels through a pertussis toxin-sensitive G protein. *Proc. Natl. Acad. Sci. USA* **92**: 8739-8743.

Patel SP and Campbell DL (2005) Transient outward potassium current, 'Ito', phenotypes in the mammalian left ventricle: underlying molecular, cellular and biophysical mechanisms. *J Physiol* **569**:7-39

Pardo LA, Heinemann SH, Terlau H, Ludewig U, Lorra C, Pongs O, and Stuhmer W (1992) Extracellular $K^+$ specifically modulates a rat brain $K^+$ channel. *Proc Natl Acad Sci USA* **89**:2466–2470

Sala F, Mulet J, Choi S, Jung SY, Nah SY, Rhim H, Valor LM, Criado M, and Sala S (2002) Effects of ginsenoside $Rg_2$ on human neuronal nicotinic acetylcholine receptors. J. Pharmacol. Exp. Ther. **301**: 1052-1059.

Sali A and Blundell TL (1993) Comparative protein modelling by satisfaction of spatial restraints. *J Mol Biol* **234**:779-815.

Salvador-Recatala V, Kim Y, Zaks-Makhina E, and Levitan ES (2006) Voltage-gated $K^+$ channel block by catechol derivatives: defining nonselective and selective pharmacophores. *J Pharmacol Exp Ther*. **319**: 758-64.

Tachikawa E, Kudo K, Nunokawa M, Kashimoto T, Takahashi E, Kitakawa S (2001)

Characterization of ginseng saponin ginsenoside-Rg$_3$ inhibition of catecholamine secretion in bovine adrenal chromaffin cells. *Biochem Pharmacol*. **62**: 943-951

Verdonk ML, Cole JC, Hartshorn MJ, Murray CW, and Taylor RD (2003) Improved protein-ligand docking using GOLD. *Proteins* **52**:609-623

Wang S, Morales MJ, Qu YJ, Bett GCL, Strauss HC, and Rasmussion RL (2003) Kv1.4 channel block by quinidine: evidence for a drug-induced allosteric effect. *J Physiol*. **546**: 387-401.

Watanabe I, Zhu J, Recio-Pinto E, and Thornhill WB (2004) Glycosylation affects the protein stability and cell surface expression of Kv1.4 but Not Kv1.1 potassium channels. A pore region determinant dictates the effect of glycosylation on trafficking. *J Biol Chem* **279**:8879-8885

Yang Y, He K, Wu T, Li Q, Zhang JS, and Fu ZG (1999) Effects of ginsenosides on myocardial reperfusion arrhythmia and lipid superoxidation in high cholesterol diet rats. *Shi Yan Sheng Wu Xue Bao*. **32**:349-352.

Zaks-Makhina E, Kim Y, Aizenman E, and Levitan ES (2004) Novel neuroprotective K$^+$ channel inhibitor identified by high-throughput screening in yeast. *Mol. Pharmacol*. **65**: 214-219

## FOOTNOTES

**Figure legends**

**Fig. 1.** Chemical structures of ginsenosides and effects of various ginsenosides on hKv1.4 channel currents. A, Ginsenosides differ in the three side chains attached to a common steroid-like ring. Abbreviations for carbohydrates are as follows: Glc, glucopyranoside; Ara (pyr), arabinopyranoside; Rha, rhamnopyranoside. Superscripts indicate the glucose ring carbon that links the two carbohydrates. B, Summary histograms showing the effects of various ginsenosides (100 µM each) on the wild-type hKv1.4 channel current. *Inset*, Representative hKv1.4 channel currents elicited by 500-ms voltage steps to +50 mV from a holding potential of −80 mV, in the absence and presence of 100-µM of ginsenosides $Rh_2$, $Rg_3$, and compound K (CK).

**Fig. 2.** $Rg_3$ effects on wild-type and mutant hKv1.4 channel currents. A, Concentration-response curves for $Rg_3$-induced inhibition of wild-type and mutant hKv1.4 channel currents. The same voltage protocol as in *A* was used to elicit the $K^+$ currents. Amino acids in outer pore residues near selectivity filter were mutated into alanine. B, Representative wild-type and K531Y mutant hKv1.4 channel currents elicited in the absence and presence of various concentrations of $Rg_3$. C, Concentration-response curves for $Rg_3$-induced inhibition of wild-type and mutant hKv1.4 channel currents. D,

Current-voltage (I-V) relationships of wild-type and mutant hKv1.4 channels in the absence or presence of Rg$_3$. Voltage pulses of 500-ms duration were applied in 10-mV increments and at 10-s intervals from a holding potential of –80 mV. The peaks of the evoked currents, normalized to the peak current evoked by the voltage step to +60 mV in the absence of Rg$_3$, were used in the I-V plot. $^*P < 0.01$ compared with wild-type hKv1.4 channel.

**Fig. 3.** Mutual antagonistic actions of extracellular [K$^+$] and Rg$_3$ on hKv1.4 channel currents. A, hKv1.4 channel currents evoked in 3-mM and 99-mM K$^+$ by 500-ms voltage pulses to +50 mV from a holding potential of 0 mV, in the absence and presence of Rg$_3$. B, Plot showing the effect of extracellular [K$^+$] on Rg$_3$ (100 μM) inhibition of the current. C, K$^+$ current activation curves constructed from the currents evoked in the absence and presence of Rg$_3$. D, I-V plots for hKv1.4 channel currents obtained in 3- and 99-mM K$^+$, in the absence and presence of Rg$_3$ (100 μM). Currents are normalized to that evoked in 3-mM K$^+$ by the voltage step to +60 mV in the absence of Rg$_3$.

**Fig. 4.** Mutually antagonistic action of TEA and Rg$_3$ on wild-type and K531Y mutant hKv1.4 channel currents. A, Concentration-dependent effects of TEA on wild-type and

K531Y hKv1.4 channel currents. B, Concentration-response curves for Rg$_3$ inhibition of the wild-type hKv1.4 channel current in the absence and presence of TEA (10 µM). *Inset*, Representative K$^+$ current traces from control oocytes (□) and oocytes treated with 100-µM Rg$_3$ + 10-µM TEA (○), or 100-µM Rg$_3$ alone (●). C, Concentration-response curves for TEA inhibition of K531Y channel currents evoked in the absence and presence of Rg$_3$ (100 µM). *Inset*, Representative K$^+$ current traces from controls (□) and oocytes treated with 100-µM Rg$_3$ + 30-µM TEA (○), or 30-µM TEA alone (●).

**Fig. 5.** Theoretical docking of Rg$_3$ to wild-type and K531Y mutant Kv1.4 channels. Hydrogen bonds are denoted as red broken lines. The Roman numerals in parenthesis indicate the number of the homotetramer subunit involved in the interaction. A, Structure of Rg$_3$. Glc, glucopyranoside. B, A docked model of wild-type Kv1.4 channel and Rg$_3$. Six hydrogen bonds are predict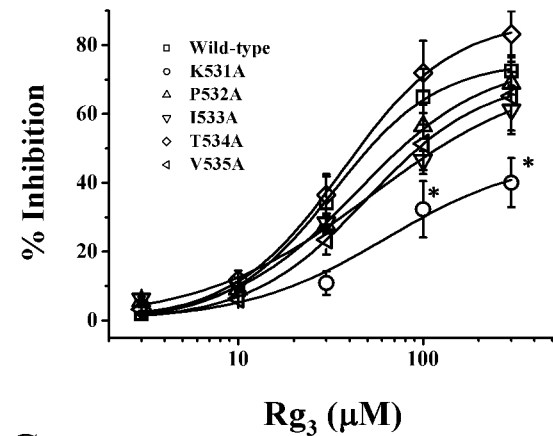ed to form between key residues and Rg$_3$, including three hydrogen bonds to K531(I) one hydrogen bond each to T505(I), His507(I), and H507(IV). The lower panel contains a 90-degree rotated view of the upper panel, showing that the Kv1.4 channel pore is predicted to be blocked by the hydrophobic triterpenoid moiety of the ginsenoside. C, A docked model showing binding of Rg$_3$ to the K531Y mutant channel. Only 2 hydrogen bonds form, one each to T531(I) and H507(IV) (see Table 2).

TABLE I

Effects of Rg$_3$ on wild-type and mutant hKv1.4 channels expressed in *Xenopus laevis* oocytes.
Currents were elicited by single-step voltage pulses from –80 to +50 mV.

| Type | IC$_{50}$ | V$_{max}$ | $n_H$ |
|---|---|---|---|
| Wild type | $32.6 \pm 2.2$ | $75.4 \pm 2.0$ | $1.59 \pm 0.13$ |
| N352Q | $38.2 \pm 3.5$ | $81.2 \pm 5.2$ | $1.61 \pm 0.22$ |
| R447C | $30.6 \pm 2.4$ | $69.1 \pm 2.1$ | $1.35 \pm 0.11$ |
| R450C | $26.1 \pm 1.1$ | $91.8 \pm 1.4$ | $1.46 \pm 0.07$ |
| L478F | $36.5 \pm 3.5$ | $93.6 \pm 3.3$ | $1.16 \pm 0.09$ |
| H507Q | $34.4 \pm 3.0$ | $84.5 \pm 2.8$ | $1.34 \pm 0.12$ |
| S510K | $39.8 \pm 1.6$ | $83.7 \pm 1.3$ | $1.25 \pm 0.04$ |
| D513Q | $41.2 \pm 3.3$ | $88.4 \pm 3.1$ | $1.32 \pm 0.21$ |
| V525L | $38.5 \pm 4.6$ | $68.1 \pm 3.1$ | $1.12 \pm 0.09$ |
| K531A | $63.3 \pm 9.4^{*}$ | $47.9 \pm 3.2^{*}$ | $1.27 \pm 0.12$ |
| K531Y | ND | ND | ND |
| P532A | $44.6 \pm 3.1$ | $75.5 \pm 2.1$ | $1.31 \pm 0.13$ |
| I533A | $39.1 \pm 7.0$ | $72.6 \pm 3.4$ | $1.31 \pm 0.12$ |
| I533M | $35.5 \pm 0.9$ | $71.5 \pm 1.8$ | $1.36 \pm 0.08$ |
| T534A | $36.9 \pm 1.6$ | $87.6 \pm 1.5$ | $1.28 \pm 0.11$ |
| V535A | $41.6 \pm 3.3$ | $70.7 \pm 2.0$ | $1.37 \pm 0.15$ |
| V535Q | $36.2 \pm 2.5$ | $72.5 \pm 4.5$ | $1.24 \pm 0.12$ |
| G548P | $29.5 \pm 5.6$ | $69.5 \pm 3.5$ | $1.26 \pm 0.23$ |
| V560A | $35.6 \pm 5.7$ | $65.8 \pm 4.1$ | $1.34 \pm 0.21$ |
| K531Y + I533M | ND | ND | ND |

ND, not determined. *$P < 0.01$ compared with wild-type hKv1.4 channel

TABLE II

Modeled hydrogen bonds between hKv1.4 and $Rg_3$.

| Type | Residue | $Rg_3$ | Distance (Å) |
|------|---------|--------|--------------|
| Wild-Type | K531 (I) | O3` | 2.336 |
| | | O2` | 2.543 |
| | | O2`` | 2.629 |
| | T505 (I) | HO4`` | 2.604 |
| | H507 (I) | O3`` | 3.288 |
| | H507 (IV) | HO4` | 2.695 |
| K531Y | Y531 (I) | HO3`` | 2.022 |
| | H507 (IV) | O3` | 2.449 |

The Roman numerals in parenthesis indicate the subunit number of the homotetramer involved in the interaction. The ` and `` markings indicate the first and second carbohydrates of $Rg_3$, respectively (see Fig. 5A), and the adjacent numbers indicate the position of the relevant carbon in each carbohydrate ring.

**A**
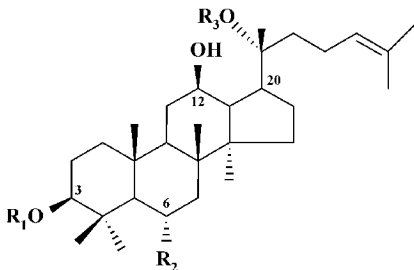


| Ginsenoside | $R_1$ | $R_2$ | $R_3$ |
|---|---|---|---|
| Rb$_1$ | -Glc$_2$-Glc | -H | -Glc$_6$-Glc |
| Rc | -Glc$_2$-Glc | -H | -Glc$_6$-Ara(fur) |
| Rd | -H | -O-Glc$_2$-Rha | -Glc |
| Rf | -H | -O-Glc$_2$-Glc | -H |
| Rg$_1$ | -H | -O-Glc | -Glc |
| Rg$_3$ | -Glc$_2$-Glc | -H | -H |
| Rh$_2$ | -Glc | -H | -H |
| CK | -H | -H | -Glc |

**B**



## Fig. 1

**Fig. 2**

**Fig. 3**

**Fig. 4**

## A. 20(*S*)-Rg₃



## B. Wild-type



20(*S*)-Rg₃

K531(I)

20(*S*)-Rg₃

H507(I)

H507(IV)

T505(I)

## C. K531Y



20(*S*)-Rg₃

Y531(I)

H507(IV)